

1 **The evolutionary dynamics of RNA-guided gene drives**

2 Charleston Noble^{*}, Jason Olejarz^{*}, ..., George M. Church & Martin A. Nowak

3 **The genetic manipulation of wild populations has been discussed as a solution to a number**
4 **of humanity's most pressing ecological and public health concerns, including the**
5 **eradication of insect-borne diseases such as malaria, the reversal of herbicide and pesticide**
6 **resistance in agriculture, and the control of destructive invasive species^{1,2}. Enabled by the**
7 **recent CRISPR/Cas9 revolution in genome editing³, RNA-guided gene drives—selfish**
8 **genetic elements which can spread through wild populations even if they confer no**
9 **advantage to their host organism—are rapidly emerging as the most promising**
10 **approach^{2,4–10}. Before this technology reaches real-world application, however, it is**
11 **imperative to develop a deep theoretical understanding of the potential long-term outcomes**
12 **of drive release in a wild population. Toward this aim, we here present the first**
13 **evolutionary dynamics study of RNA-guided gene drives. In particular, we show that drive**
14 **spread occurs along one of four distinct classes of trajectories—two of which are**
15 **counterintuitive and previously unreported—and we derive simple conditions based on**
16 **tunable design parameters which are sufficient to yield evolution toward a desired**
17 **outcome. Furthermore, our results imply a simple design for ‘threshold gene drives’ which**
18 **spread only if released at a sufficiently high initial frequency, providing a practical**
19 **mechanism for localized containment of gene drive spread^{11–13}.**

20 Gene drives are selfish genetic elements which bias their own inheritance and spread
21 through populations in a super-Mendelian fashion (Fig. 1a). Various examples can be found in
22 nature, including transposons¹⁴, Medea elements¹⁵, and segregation distorters¹⁶, but so-called

^{*}These authors contributed equally to this work

23 homing endonuclease gene drives have received the most significant attention in the literature. In
24 general, these function by converting drive-heterozygotes into homozygotes through a two-step
25 process: (1) the drive construct, encoding a sequence-specific endonuclease, induces a double-
26 strand break (DSB) at its own position on a homologous chromosome, and (2) subsequent DSB
27 repair by homologous recombination (HR) copies the drive into the break site (Fig. 1b). Any
28 sequence adjacent to the endonuclease will be copied as well; if a gene is present we refer to it as
29 ‘cargo’, as it is ‘driven’ by the endonuclease through the population.

30 Though originally proposed over a decade ago¹, the chief technical difficulty of this
31 approach—inducing precisely targeted cutting—has only recently been overcome by the
32 discovery and development of the CRISPR/Cas9 system^{3,17}. Briefly, Cas9 is an endonuclease
33 whose target site is prescribed by an independently expressed guide RNA (gRNA) via a 20-
34 nucleotide protospacer sequence. Due to the large space of possible 20-nucleotide sequences,
35 virtually any position in a genome can be uniquely targeted by Cas9, and thus so-called RNA-
36 guided gene drives can be constructed simply, requiring only the engineering of a suitable
37 Cas9/gRNA construct².

38 Previous studies have provided experimental proofs-of-concept for endonuclease gene
39 drives in small laboratory populations^{4-7,18} or considered the population genetics of gene drives
40 under specific conditions^{1,19,20}, but none have explored the evolutionary dynamics of gene drives
41 in general. Of particular concern is the potential for emergence of drive resistance within a
42 population, which has not been studied in any depth previously. This can occur if non-
43 homologous end joining (NHEJ) is employed rather than HR in repairing a drive-induced
44 double-strand break; this pathway typically introduces a small insertion-deletion mutation at the
45 endonuclease target sequence, resulting in the creation of a drive-resistant allele rather than the

46 desired duplication of the drive allele (Fig. 1b). Far from an unlikely scenario, NHEJ is strongly
47 favored over HR in many organisms²¹⁻²³.

48 To understand the potential behaviors of RNA-guided gene drives, we here consider a
49 genetics-based evolutionary dynamics model. In particular, we study the evolution of a
50 population of diploid organisms and focus on a specific locus which has three alleles, the wild-
51 type (A), the gene drive (D), and a drive-resistant allele (R) which is a loss-of-function variant of
52 the wild-type (Fig. 1b). To abstract the cellular-level drive dynamics, we assume that the wild-
53 type allele in an AD heterozygote is converted to a drive allele with probability P or to a drive-
54 resistant allele with probability 1-P (Fig. 1c). Both the drive and resistant alleles are immune to
55 targeting by the endonuclease and thus are not converted similarly. A simple biological
56 interpretation for P is the chance that double-strand break repair occurs by HR rather than NHEJ,
57 and this varies from as low as $P \approx 0.25$ in mammalian cells²³ to as high as $P \approx 1$ in yeast^{5,24}.

58 To describe the population-level dynamics of gene drive spread, we assume that gene
59 drive release occurs in an infinite, randomly mating population with viability selection. For the
60 sake of simplicity, we assume that the drive confers a dominant fitness cost c on its host
61 organism, while the resistant allele confers a recessive cost s (Fig. 1d). We consider the former
62 justified by the high cutting efficiency of Cas9 paired with its potential for off-target cleavage³
63 and the latter by the relative rarity of dominant loss-of-function mutations²⁵. Note that both of
64 these parameters can be tuned when engineering gene drive systems: c can be increased either by
65 including a costly (dominant) cargo gene in the drive construct or by engineering purposeful off-
66 target cleavage, while s can be increased or decreased simply by choosing more- or less-
67 essential genes for targeting by the drive.

68 Depending on these costs, gene drive release in a population results in one of four long-
69 term behaviors (Fig. 2). Each occurs in a distinct regime in parameter space, and these are
70 separated by simple, linear boundaries: $s=c$ and $c=P/(1+P)$ (Fig. 2a and 2b). The former
71 intuitively divides the space based on whether the drive allele or resistant allele is more costly,
72 while the latter can roughly be thought of as the minimum cost for which the drive no longer
73 achieves super-Mendelian inheritance. To see this, consider an AD heterozygote. If D were to
74 follow standard Mendelian inheritance, then the next generation would inherit it with probability
75 $P_M=1/2$. If, instead, D were a gene drive as described above, then the next generation would
76 inherit it with probability $P_D=(1-c)(1+P)/2$. Super-Mendelian inheritance then requires that
77 $P_D>P_M$, implying that $(1-c)(1+P)>1$, or equivalently, $c<P/(1+P)$.

78 Two of these regimes, I and IV, produce the expected dynamics. If the drive is fairly
79 neutral and resistance is costly (Regime I), then the drive eventually spreads to fixation (Fig. 2c
80 and Fig. 3a). Resident wild-type populations are susceptible to invasion by infinitesimal initial
81 drive perturbations (SI Sections 3.1 and 3.4), and near fixation, the drive is itself resistant to
82 invasion (SI Sections 3.2 and 3.5). Furthermore, fully-resistant populations are also susceptible
83 (SI Sections 3.3 and 3.6), implying that the drive wins in any resident population. If,
84 alternatively, the drive is costly and resistance is less costly (Regime IV), both the gene drive and
85 resistant alleles go extinct (Fig. 2c and 3d). More precisely, wild-type populations are immune to
86 invasion (SI Sections 3.1 and 3.4), while drive populations are susceptible to invasion by the
87 resistant allele (SI Sections 3.2 and 3.5), and resistant populations are susceptible to invasion by
88 the wild-type allele (SI Sections 3.3 and 3.6).

89 The other two regimes, II and III, yield counterintuitive and previously unreported
90 behavior. Of particular interest is Regime II, wherein the drive is costly but resistance is costlier.

91 Here we observe what we term threshold-dependent drive fixation (Fig. 2c and Fig. 3b). If the
92 drive is introduced at a sufficiently high frequency in a wild-type population, it goes to fixation,
93 otherwise the population returns to its initial wild-type state. Mathematically, this is due to
94 bistability: wild-type populations are immune to invasion (SI Sections 3.1 and 3.4), but so are
95 populations with a fixed drive allele (SI Sections 3.2 and 3.5). The boundary between these two
96 behaviors then manifests itself as a threshold (which we refer to as the ‘invasion threshold’) (Fig.
97 2c). On the other hand, if the drive is fairly neutral with resistance even more-so (Regime III),
98 then we observe coexistence of all three alleles (Fig. 2c and Fig. 3c). This behavior can again be
99 explained by the stability of the various fixed points—each allele, at fixation, is susceptible to
100 invasion by at least one of the other alleles (SI Sections 3.1-3.6). Regardless of initial conditions,
101 the system spirals into an interior fixed point (given in SI Section 5) which appears to be stable.

102 Next we consider how these dynamics vary within the regimes themselves. Toward this
103 aim, we have taken the two most useful regimes—I and II—and studied their most salient
104 features: the speed of drive spread (Fig. 4a) and the invasion threshold (IT) (Fig. 4b). To quantify
105 the former, we calculate the time before the drive allele reaches a frequency of 90%, which we
106 denote t_{90} . Intuitively, this decreases as the drive becomes more neutral and as resistance
107 becomes more costly (Fig. 4a), while increasing the conversion probability P increases the size
108 of the regime over which fixation occurs (Fig. 2b) and speeds up drive fixation for set costs (Fig.
109 4a). The invasion threshold in Regime II is less intuitive: the resistance cost affects whether the
110 threshold behavior occurs at all but does not appreciably affect the value of the threshold (Fig.
111 4b), while the threshold does increase with the drive cost, from nearly $IT=0$ at the lower
112 boundary ($c=P/(1+P)$) to $IT=1$ as the drive approaches lethality ($c=1$). Again, the conversion
113 probability P simply determines the size of the regime over which threshold behavior occurs.

114 Our results suggest that gene drive resistance—not considered in any depth previously—
115 must be thoroughly understood before the technology reaches real-world application. Most
116 important is the possibility of ‘cost-free resistance’. If an organism evolves resistance through a
117 mechanism which bears no cost, for example a synonymous mutation in the Cas9 protospacer
118 sequence, a fourth allele will emerge which is constrained to the horizontal ($s=0$) axis in Figure
119 2a, and this allele will always out-compete the gene drive at equilibrium. Indeed, this effect—
120 drive fixation followed by extinction—has been observed in taxonomic and phylogenetic
121 analyses of natural homing endonuclease genes^{26,27}. To address this problem, drive resistance
122 could likely be delayed, although not entirely precluded, by the use of an RNA-guided gene
123 drive system employing multiple guide RNAs which all target a particular locus, as suggested by
124 Esvelt et al². If cutting were induced by two or more guides simultaneously, then repair by NHEJ
125 would result in a loss of the intervening sequence and disrupt target gene function. This strategy,
126 while intuitively appealing, should be validated by further theoretical study.

127 In contrast to the canonical goal of gene drives—to spread as effectively as possible—
128 there are also applications for which containment to a local population is required. For example,
129 the mosquito *Culex quinquefasciatus* is invasive to Hawaii and, as the principal vector for avian
130 malaria, has been implicated in the extinction of a variety of endemic avian species²⁸. Thus it
131 might be a desirable goal to locally eradicate or otherwise modify Hawaiian *C. quinquefasciatus*
132 without affecting its native populations elsewhere. Toward this aim, a gene drive system could
133 be engineered to exist in our Regime II (Fig. 2 and Fig. 3b) and would naturally constitute a
134 threshold drive: assuming that the flux of mosquitos from Hawaii to other populations is
135 sufficiently low, any escaped drive allele would go extinct upon arrival. Previously considered
136 methods for constructing such drives—based on engineered underdominance or toxin-antidote

137 systems—require high introduction frequencies to spread in the intended population and ignore
138 the problem of drive resistance^{11,12}; thus we believe our method to be a significant advance
139 toward the engineering of threshold-based gene drives.

140 **Methods**

141 **Evolutionary dynamics model**

142 Throughout this work we study a genetics-based evolutionary dynamics model; to avoid making
143 any explicit allele frequency assumptions, we first consider the evolution of six types of diploid
144 individuals, x_{AA} , x_{DD} , x_{RR} , x_{AD} , x_{RD} , and x_{RA} , where A, D, and R correspond to the wild-type,
145 gene drive, and resistant alleles as described above. We enforce a density constraint such that, at
146 any given time, the total number of individuals sums to one. In this way, we track the frequencies
147 of the various individuals rather than their total abundances.

148 In the Supplementary Information (Section 1) we derive a continuous-time model for the
149 evolutionary dynamics of this population assuming (1) an infinitely large population, (2) random
150 mating, (3) standard segregation of allele pairs at meiosis, unless an individual is AD, in which
151 case gametes receive a D allele with probability $\frac{1}{2}(1+P)$ or an R allele with probability $\frac{1}{2}(1-P)$,
152 and (4) selection dynamics as described in Fig. 1d. This continuous-time model makes no
153 explicit assumptions regarding allele frequencies, but our simulations show that it is equivalent
154 to a simpler model (derived from the individual-based model) where we instead track the allele
155 frequencies with explicit Hardy-Weinberg frequency assumptions; this suggests that the
156 assumptions are valid, and thus we consider the allele-based model throughout the results
157 presented in the main text, reducing the dimensionality of the system from five (six types of
158 individuals with the density constraint) to two (three alleles with a density constraint).

159 In this simpler model, we consider the frequencies of the A, D, and R alleles, denoted p,
 160 q, and r respectively. In continuous time, these follow

$$\begin{aligned}\frac{dp}{dt} &= \varphi[p^2 + pr - \varphi p] \\ \frac{dq}{dt} &= \varphi[(1 - c)(1 + P)pq + (1 - c)q^2 + (1 - c)rq - \varphi q] \\ \frac{dr}{dt} &= \varphi[(1 - c)(1 - P)pq + (1 - s)r^2 + (1 - c)rq + rp - \varphi r],\end{aligned}$$

161 where φ is chosen to enforce our density constraint $p+q+r=1$.

162 **Invasion and stability of fixed points**

163 To the system of differential equations above, we make the substitution $p=1-q-r$. Then the
 164 (autonomous) system above is described by

$$\begin{cases} \frac{dq}{dt} = f_q(q, r) \\ \frac{dr}{dt} = f_r(q, r). \end{cases}$$

165 We Taylor expand to linearize the system near a given fixed point (q^*, r^*) and consider the
 166 Jacobian, given by

$$J_{(q^*, r^*)} = \begin{pmatrix} \left. \frac{\partial f_q}{\partial q} \right|_{(q^*, r^*)} & \left. \frac{\partial f_q}{\partial r} \right|_{(q^*, r^*)} \\ \left. \frac{\partial f_r}{\partial q} \right|_{(q^*, r^*)} & \left. \frac{\partial f_r}{\partial r} \right|_{(q^*, r^*)} \end{pmatrix}.$$

167 To determine the conditions for which allele invasion occurs in various resident populations, we
 168 then perform linear stability analysis of fixed points via consideration of the eigenvalues of the
 169 Jacobian. In particular, we consider the fixed points corresponding to wild-type fixation (0,0),

170 drive fixation (1,0), and resistant allele fixation (0,1). When an eigenvalue is zero and linear
171 stability analysis is inconclusive, we also perform perturbation analysis to determine the invasion
172 conditions (see Supplementary Information).

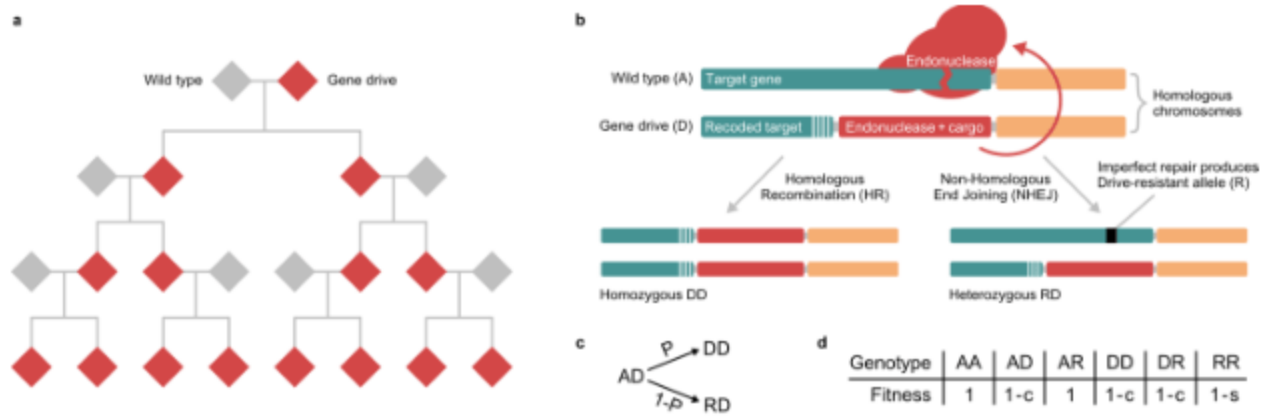
173 **Parameter values for main text figures**

174 Fig. 2a: an intermediate conversion probability was chosen, $P=0.5$. Fig. 2c: the conversion
175 probability P was as in panel a, $P=0.50$. Cost parameters were chosen to most clearly illustrate
176 the behaviors in the four regimes. Regime I: $c=0.20$, $s=0.55$, Regime II: $c=0.40$, $s=0.55$, Regime
177 III: $c=0.15$, $s=0.09$, Regime IV: $c=0.40$, $s=0.09$. Fig. 3: here all parameters are as in Fig. 2c, with
178 initial drive frequencies q_0 as follows. Regime I: $q_0=0.01$, Regime II: $q_0=0.20$ and $q_0=0.40$,
179 Regime III: $q_0=0.01$, Regime IV: $q_0=0.40$. In each case, we set the initial wild-type allele
180 frequency to one minus the initial drive frequency with no resistant allele. Fig. 4, Top: all
181 parameters were chosen identically to the corresponding panels (Regime I and Regime II) in Fig.
182 3. Middle: $P=0.25$, Bottom: $P=0.90$. Throughout panel a, we use $q_0=0.01$. In Fig. 4b, we
183 determined the invasion threshold for each (c,s) pair using a binary search-type numerical
184 algorithm which identifies the threshold down to a resolution of r ($r=0.01$). More precisely, we
185 initialize variables $L=0$ and $U=1$ and run a simulation with an initial drive frequency mid-way
186 between U and L , $q_0=(U-L)/2$ (with the initial wild-type frequency being $1-q_0$). If after $T=200$
187 the drive frequency is higher than its initial value, we consider q_0 to be above the threshold and
188 set $U=(U-L)/2$. Otherwise we consider q_0 to be below the threshold and set $L=(U-L)/2$. The
189 algorithm then continues recursively until $|L-U|<r$, at which point we make the approximation
190 that the threshold occurs at $q_0=(U-L)/2$.

191

- 192 1. Burt, A. Site-specific selfish genes as tools for the control and genetic engineering of
193 natural populations. *Proc. Biol. Sci.* **270**, 921–928 (2003).
- 194 2. Esvelt, K. M., Smidler, a. L., Catteruccia, F. & Church, G. M. Concerning RNA-guided
195 gene drives for the alteration of wild populations. *Elife* **3**, e03401 (2014).
- 196 3. Mali, P., Esvelt, K. M. & Church, G. M. Cas9 as a versatile tool for engineering biology.
197 *Nat. Methods* **10**, 957–63 (2013).
- 198 4. Gantz, V. M. & Bier, E. The mutagenic chain reaction: A method for converting
199 heterozygous to homozygous mutations. *Science (80-.)*. (2015).
200 doi:10.1126/science.aaa5945
- 201 5. DiCarlo, J. E., Chavez, A., Dietz, S. L., Esvelt, K. M. & Church, G. M. *RNA-guided gene*
202 *drives can efficiently bias inheritance in wild yeast.* *bioRxiv* (Cold Spring Harbor Labs
203 Journals, 2015). doi:10.1101/013896
- 204 6. Windbichler, N. *et al.* A synthetic homing endonuclease-based gene drive system in the
205 human malaria mosquito. *Nature* **473**, 212–215 (2011).
- 206 7. Windbichler, N. *et al.* Homing endonuclease mediated gene targeting in *Anopheles*
207 *gambiae* cells and embryos. *Nucleic Acids Res.* **35**, 5922–33 (2007).
- 208 8. Gurwitz, D. Gene drives raise dual-use concerns. *Science (80-.)*. **345**, 1010 (2014).
- 209 9. Oye, K. A. *et al.* Regulating gene drives. *Science (80-.)*. **345**, 626–8 (2014).
- 210 10. Akbari, B. O. S. *et al.* Safeguarding gene drive experiments in the laboratory. *Science (80-*
211 *)*. science.aac7932– (2015). doi:10.1126/science.aac7932
- 212 11. Akbari, O. S. *et al.* A synthetic gene drive system for local, reversible modification and
213 suppression of insect populations. *Curr. Biol.* **23**, 671–7 (2013).
- 214 12. Marshall, J. M. & Hay, B. a. Confinement of gene drive systems to local populations: A
215 comparative analysis. *J. Theor. Biol.* **294**, 153–171 (2012).
- 216 13. Sinkins, S. P. & Gould, F. Gene drive systems for insect disease vectors. *Nat. Rev. Genet.*
217 **7**, 427–435 (2006).
- 218 14. Charlesworth, B. & Langley, C. H. The population genetics of *Drosophila* transposable
219 elements. *Annu. Rev. Genet.* **23**, 251–287 (1989).
- 220 15. Chen, C.-H. *et al.* A Synthetic Maternal-Effect Selfish Genetic Element Drives Population
221 Replacement in *Drosophila*. *Science (80-.)*. **316**, 597–600 (2007).
- 222 16. Lyttle, T. W. Segregation distorters. *Annu. Rev. Genet.* **25**, 511–557 (1991).

- 223 17. Mali, P. *et al.* RNA-guided human genome engineering via Cas9. *Science* **339**, 823–6
224 (2013).
- 225 18. Simoni, A. *et al.* Development of synthetic selfish elements based on modular nucleases in
226 *Drosophila melanogaster*. *Nucleic Acids Res.* **42**, 7461–72 (2014).
- 227 19. Deredec, A., Burt, A. & Godfray, H. C. J. The population genetics of using homing
228 endonuclease genes in vector and pest management. *Genetics* **179**, 2013–2026 (2008).
- 229 20. Deredec, A., Godfray, H. C. J. & Burt, A. Requirements for effective malaria control with
230 homing endonuclease genes. *Proc. Natl. Acad. Sci. U. S. A.* **108**, E874–80 (2011).
- 231 21. Khanna, K. K. & Jackson, S. P. DNA double-strand breaks: signaling, repair and the
232 cancer connection. *Nat. Genet.* **27**, 247–254 (2001).
- 233 22. Vilenchik, M. M. & Knudson, A. G. Endogenous DNA double-strand breaks: production,
234 fidelity of repair, and induction of cancer. *Proc. Natl. Acad. Sci. U. S. A.* **100**, 12871–
235 12876 (2003).
- 236 23. Mao, Z., Bozzella, M., Seluanov, A. & Gorbunova, V. Comparison of nonhomologous
237 end joining and homologous recombination in human cells. *DNA Repair (Amst)*. **7**, 1765–
238 71 (2008).
- 239 24. DiCarlo, J. E. *et al.* Genome engineering in *Saccharomyces cerevisiae* using CRISPR-Cas
240 systems. *Nucleic Acids Res.* **41**, 4336–43 (2013).
- 241 25. Griffiths, A. J. F. *An Introduction to Genetic Analysis*. (W. H. Freeman, 2005). at
242 <<https://books.google.com/books?hl=en&lr=&id=qtboPf9eeUkC&pgis=1>>
- 243 26. Burt, A. & Koufopanou, V. Homing endonuclease genes: the rise and fall and rise again of
244 a selfish element. *Curr. Opin. Genet. Dev.* **14**, 609–15 (2004).
- 245 27. Goddard, M. R. & Burt, A. Recurrent invasion and extinction of a selfish gene. *Proc. Natl.*
246 *Acad. Sci.* **96**, 13880–13885 (1999).
- 247 28. Iii, C. V. R., Riper, S. G. Van, Goff, M. L. & Laird, M. The Epizootiology and Ecological
248 Significance of Malaria in Hawaiian Land Birds. *Ecol. Monogr.* **56**, 327–344 (1986).



249

250 **Figure 1 | Endonuclease gene drives undergo biased inheritance in wild populations.** **a**, Matings between wild
 251 type (AA) and gene drive (DD) individuals yield homozygous DD offspring, allowing for rapid spread of the gene
 252 drive allele. **b**, This is accomplished by conversion of heterozygous AD cells to homozygous DD cells in the early
 253 embryo or late germline. The gene drive carries an endonuclease (red) which cuts the wild type allele at its own
 254 position on a homologous chromosome (blue). Homologous recombination (HR) then uses the drive chromosome as
 255 a template to repair the break, inserting a new drive construct at the break site. Alternatively, repair by non-
 256 homologous end joining (NHEJ) produces a small insertion/deletion mutation, protecting the site from future
 257 recognition by the endonuclease. **c**, Our model abstracts this process using a parameter P which is roughly the
 258 probability of repair by HR. **d**, We assume that the gene drive has a dominant fitness cost c , while resistant alleles
 259 have a recessive fitness cost s .

260

261

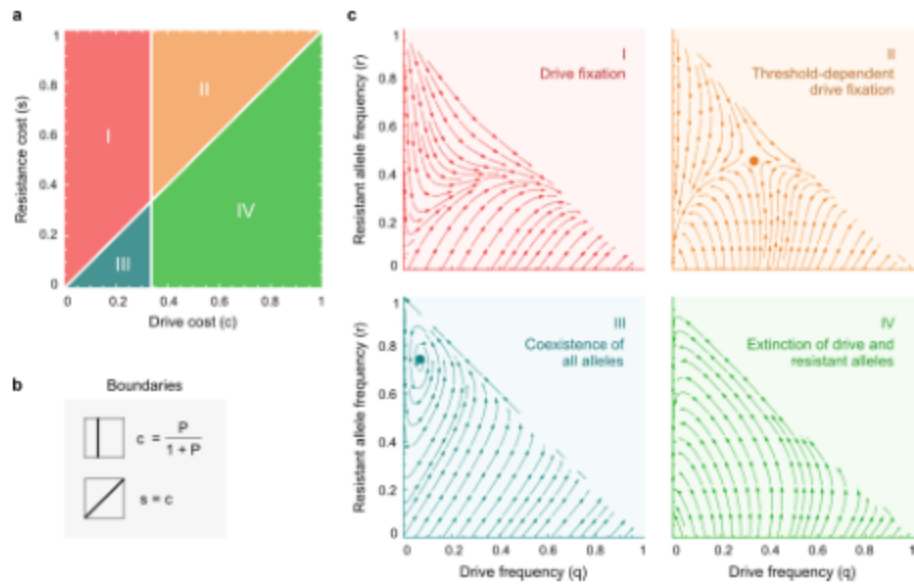
262

263

264

265

266



267

268 **Figure 2 | The relative fitness costs of the gene drive (c) and the resistant allele (s) determine four distinct**
 269 **long-term behaviors.** **a**, Phase diagram depicting the regimes in which each of the four behaviors occur. **b**, The

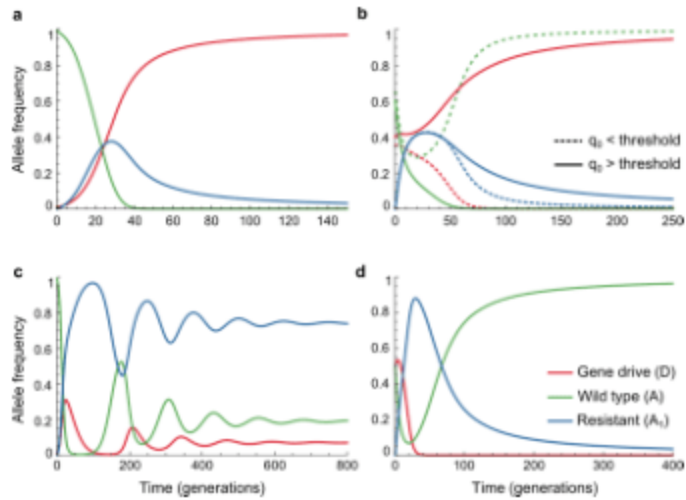
270 phase boundaries in **a**. The vertical boundary is determined by the probability of successful repair by HR, while the
 271 diagonal boundary divides the space based on which fitness cost is greater. **c**, Representative phase portraits for each
 272 regime.

273

274

275

276



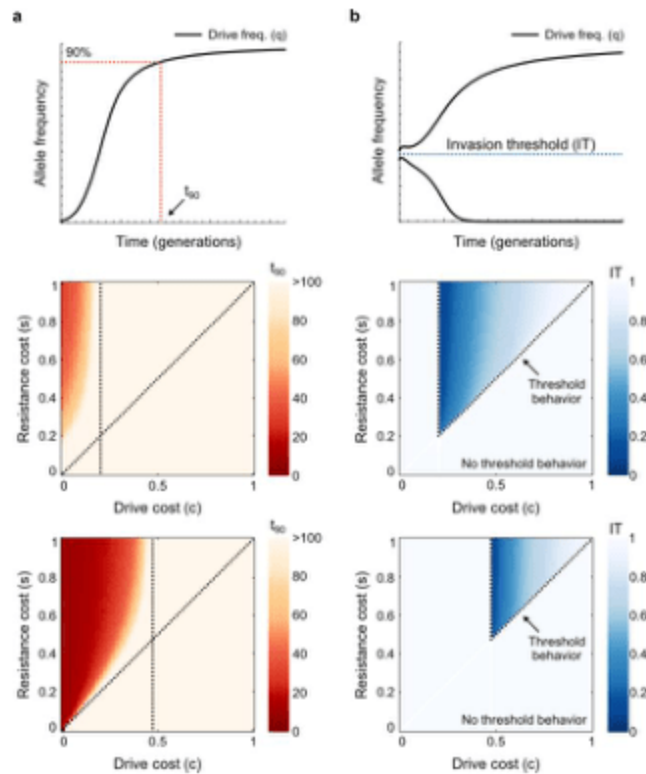
277

278 **Figure 3 | The four regimes in Fig. 2 produce diverse dynamic behaviors.** Example simulations depicting allele
 279 frequencies of the gene drive (red), wild-type (green), and resistant alleles (blue) for each of the regimes in Fig. 2. **a**
 280 through **d** demonstrate Regimes I through IV, respectively. In **b**, two simulations are depicted: one with an initial
 281 gene drive frequency below the invasion threshold (dashed lines) and one above (solid lines).

282

283

284



285

286 **Figure 4 | The speed of gene drive spread and the invasion threshold are both tunable based on the fitness**
 287 **costs of the gene drive (c) and the resistant allele (s).** a, The time (in generations) before a gene drive reaches a
 288 frequency of 90%, denoted t_{90} (illustrated at top, red). Pictured below are heat maps of t_{90} as a function of the drive
 289 cost and resistance cost for organisms having low (middle, $P = 0.25$) or high HR rates (bottom, $P = 0.90$). b, The
 290 invasion threshold, denoted IT, for drives in Regime II (illustrated at top, blue). Below are heat maps for organisms
 291 with low (middle, $P = 0.25$) or high HR rates (bottom, $P = 0.90$). Dashed black lines represent the regime boundaries
 292 in Fig. 2b.